JOURNAL OF SOLID STATE CHEMISTRY 112, 9–14 (1994)

On the Vibrational Spectra and Structure of $FeCrO_3$ and of the Ilmenite-Type Compounds $CoTiO_3$ and $NiTiO_3$

M. I. Baraton,* G. Busca,†,[1] M. C. Prieto,‡ G. Ricchiardi,† and V. Sanchez Escribano‡

*Laboratoire de Materiaux Ceramiques et Traitement de Surface, URA CNRS 320, Université, 123 Ave. A. Thomas, F-87060 Limoges, France; †Istituto di Chimica, Facoltà di Ingegneria, Università, P.le Kennedy, I-16129 Genova, Italy; and ‡Departamento de Quimica Inorganica, Facultad de Quimica, Universidad, E-37008 Salamanca, Spain

Received June 21, 1993; in revised form October 11, 1993; accepted October 21, 1993

The XRD patterns and the IR and Raman spectra of fine powders of the corundum-type sesquioxides α-Fe_2O_3 and α-Cr_2O_3, of the ilmenite-type mixed oxides $NiTiO_3$ and $CoTiO_3$, and of the mixed oxide α-$FeCrO_3$ is obtained from the XRD pattern, the IR and Raman spectra provide evidence for the centrosymmetric ilmenite-type superstructure in the case of α-$FeCrO_3$. The noncentrosymmetric alternative superstructure ($LiNbO_3$-like) is excluded by the validity of the mutual exclusion rule. © 1994 Academic Press, Inc.

INTRODUCTION

The thermodynamically stable forms of the sesquioxides of iron and chromium (hematite and eskolaite, respectively) are isostructural with each other and with corundum (1). They are miscible, giving rise to thermodynamically stable solid solutions in the entire compositional range that retain the hexagonal structure of the parent binary oxides (2). Materials with this composition can also be produced as fine powders by coprecipitation methods (3). These mixed oxide powders hold interest for the fields of heterogeneous catalysis (they constitute active phases of the high-temperature water–gas shift catalysts and are components of dehydrogenation and oxidative dehydrogenation catalysts (4–6)), and of pigment, sensor, and adsorbant technologies (7).

The characterization of iron–chromium mixed oxides finds relevance also in the field of corrosion science. In fact, they can be formed as corrosion products of stainless steel. Raman spectroscopy is largely used for this purpose. Due to the detection of a strong Raman band near 650–700 cm^{-1}, normally present in spinel compounds but absent in corundum-type compounds, some authors concluded that stainless steel oxidizes in the form of the $FeCr_2O_4$ spinel (8, 9). However, McCarty and Boehme (10) reported that a strong band in the same position is also present in the Raman spectra of $Fe_{2-x}Cr_xO_3$ solid solutions with corundum-type structure.

We prepared high-area binary and ternary oxides with related hexagonal structures in order to complete our studies of the surface chemistry of metal oxide systems of catalytic interest (3, 11–13). We report here a vibrational characterization of $FeCrO_3$ fine powders. In particular, we will compare the spectra of this compound with those of the mixed oxides $NiTiO_3$ and $CoTiO_3$, whose structure, of the ilmenite type, is closely related. A comparison of these data will allow us to have information on the structure of these compounds.

EXPERIMENTAL

The preparation of $Fe_{2-x}Cr_xO_3$ mixed oxides has been described in a previous paper (3). They were obtained by coprecipitation from mixed solutions of the corresponding nitrates. $NiTiO_3$ and $CoTiO_3$ were prepared by adding $Ti(OCH(CH_3)_2)_4$ to a concentrated solution of Ni (or Co) nitrate. The water was later evaporated and the cake dried. Finally, the powder was calcined at 973 K for 3 hr.

IR spectra were recorded with a Bomem MB-102 spectrometer in the 4000–200 cm^{-1} range and 4 cm^{-1} resolution. The powders have been pressed into CsI standard pellets (concentration 0.6–0.9% w/w). Raman scattering measurements were carried out with a Dilor microprobe with a double monochromator and using 514.5 Ar ion laser radiation.

RESULTS AND DISCUSSION

The XRD powder diffraction peaks of the materials under study are reported in Tables 1 and 2, where they are also compared with those of corundum and ilmenite-type phases as reported in the JCPDS tables. The XRD patterns of α-$FeCrO_3$, α-Fe_2O_3, and α-Cr_2O_3 powders, already discussed previously (3), are very similar to each other and show a progressive displacement, in the sense

[1] To whom correspondence should be addressed.

0022-4596/94 $6.00

TABLE 1
XRD Peak Position (*A*) of Oxide Materials and of Reference Compounds

	d				
hkl	α-Fe_2O_3[a]	α-Fe_2O_3	α-$FeCrO_3$	α-Cr_2O_3	α-Cr_2O_3[b]
012	3.6836	3.697	3.700	3.629	3.6312
104	2.7001	2.712	2.695	2.661	2.6649
110	2.5191	2.522	2.525	2.474	2.4794
113	2.2069	2.210	2.204	2.166	2.1753
024	1.8409	1.844	1.838	1.810	1.8156
116	1.6940	1.695	1.684	1.672	1.6725
018	1.5994	1.601	1.595	1.574	—
214	1.4857	1.488	1.478	1.461	1.4649
300	1.4540	1.454	1.450	1.434	1.4317
			Cell parameters (*A*)		
a	5.0356	5.03(1)	4.99(2)	4.96(3)	4.954
c	13.7489	13.73(3)	13.62(7)	13.56(7)	13.584

[a] JCPDS file 33-664.
[b] JCPDS file 38-1479.

of a contraction of the cell parameters by increasing Cr content and decreasing Fe content. It is evident that the corundum-type structure of the two sesquioxides is retained by the mixed oxide, while a superstructure is not apparent. This could be interpreted, according to literature data (1,14), as evidence that cation ordering does not occur, their distribution being random in the same sites occupied in the corundum-type structure. This should result in the retention of the $R\bar{3}c = D_{3d}^6$ space group characterizing the corundum-type structure.

The XRD patterns of the ilmenite-type phases $NiTiO_3$ and $CoTiO_3$ (Table 2) are also qualitatively very similar to those of iron and chromium oxides. However, we can observe evidence of a superstructure in these cases according to the detection of additional XRD peaks, absent for corundum-type sesquioxides (Table 1).

The IR spectra of these compounds are reported in Figs. 1 and 2. The spectra of the two pure sesquioxides, α-Fe_2O_3 and α-Cr_2O_3, agree with those of similar powders, reported by Serna *et al.* (15). The comparison with single-crystal reflection spectra (16) is not very easy because of the apparent sensitivity of some bands to the extent of crystallinity, as pointed out by Yariv and Mendelovici (17), and because of the complexity arising from the particle morphologies. In the spectrum of hematite powders, we observe three bands, certainly due to IR fundamentals, at 529, 444, and 308 cm^{-1}, and a weaker one near 392 cm^{-1}, while for eskolaite we observe sharp bands at 628, 562, 444, and 409 cm^{-1}. According to Serna *et al.* (15), the shoulders observed at 635 cm^{-1} in the spectrum of Fe_2O_3 and near 700 cm^{-1} in that of Cr_2O_3 are components of the higher frequency fundamental TO modes (529 and 628 cm^{-1} for α-Fe_2O_3 and α-Cr_2O_3, respectively) shifted

TABLE 2
XRD Peak Position (*A*) of Oxide Materials and of Reference Compounds

	d					
hkl	α-Fe_2O_3	$MgTiO_3$	$NiTiO_3$	$NiTiO_3$	$CoTiO_3$	$CoTiO_3$
003		4.64	4.5971			4.61
101		4.18				
012	3.6836	3.703	3.6835	3.6769	3.717	3.6956
104	2.7001	2.722	2.7054	2.7011	2.727	2.7154
110	2.5191	2.527	2.5160	2.5103	2.5340	2.5236
015			2.3326			
006			2.2985	2.2986	2.3202	
113	2.2069	2.218	2.2069	2.2038	2.2240	2.2162
202		2.090	2.0771	2.0829	2.0934	2.0835
024	1.8409	1.852	1.8417	1.8388	1.8566	1.8507
107		1.809	1.7949		1.8114	
116	1.6940	1.708	1.6961	1.6948	1.7114	1.7062
211		1.6434	1.6351	1.6222		1.6453
018	1.5994	1.6148	1.6025	1.6006	1.6159	1.6129
214	1.4857	1.4938	1.4857	1.4844	1.4974	1.4942
300	1.4540	1.4592	1.4520	1.4506	1.4628	1.4594
	[a]	[b]	[c]	This work	[d]	This work
			Cell parameters (*A*)			
a	5.0356	5.054	5.0302	5.027(3)	5.0683	5.065(3)
c	13.7489	13.898	13.7905	13.78(1)	13.9225	13.907(8)

[a] JCPDS file 33-664.
[b] JCPDS table 6-0494.
[c] JCPDS table 33-0960.
[d] JCPDS table 15-866.

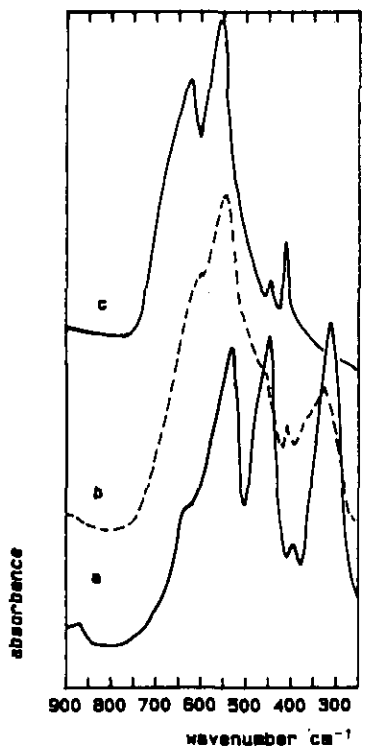

FIG. 1. FT–IR spectra (CsI pressed disks) of (a) α-Fe_2O_3, (b) $FeCrO_3$, and (c) α-Cr_2O_3.

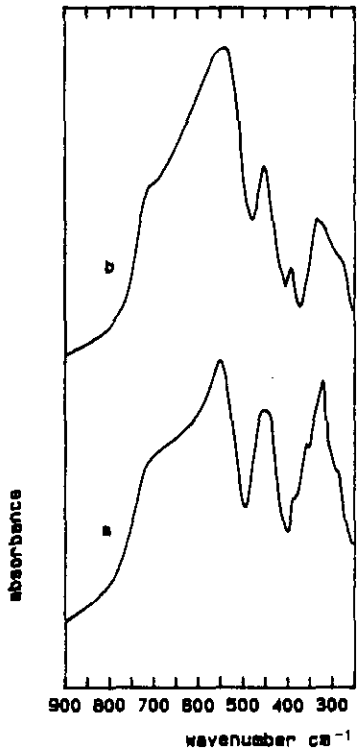

FIG. 2. FT–IR spectra (CsI pressed disks) of (a) $NiTiO_3$ and (b) $CoTiO_3$.

upward toward the value of the corresponding LO mode as an effect of particle morphology.

The spectrum of α-$FeCrO_3$ shows components at 610, 551, 465, 410, and 328 cm^{-1} with additional shoulders near 700, 500, and 350 cm^{-1}. This spectrum is similar to those reported by Gillot *et al.* (18) for similar solid solutions. We can only conclude that the spectrum is apparently slightly more complex than those of the two parent oxides, although it is less resolved.

The IR spectra of the ilmenite-type mixed oxides (Fig. 2) show a general similarity with those of corundum-type sesquioxides. For $NiTiO_3$ we observe three strong bands as for Fe_2O_3 at 555, 453, and 321 cm^{-1}, although components are also evident at 705, 380, 350, and 300 cm^{-1}. The spectrum of $CoTiO_3$ shows a pronounced similarity, in relation to the shape and the position of the bands, with that of $FeCrO_3$, although with a better resolution. The peaks are observed at 539, 445, 385, and 327 cm^{-1}, with pronounced shoulders at 709 and 270 cm^{-1}. These spectra are similar to those reported in the literature for the isostructural compounds ilmenite $FeTiO_3$ (19) and $ZnTiO_3$ (20). In conclusion, the IR spectra of all these compounds show a significant parallelism.

In contrast, the Raman spectra of the mixed oxides $NiTiO_3$ and $CoTiO_3$, as well as of $FeCrO_3$, are similar to each other but differ greatly from those of the two sesquioxides, which incidentally, are also very different from each other as the peak intensities are concerned. The Raman spectra we measured for α-Fe_2O_3 and α-Cr_2O_3 (Fig. 3) are very similar to those reported by several authors (10, 21–23). For hematite we observe peaks at 596, 490, 395, 281, and 217 cm^{-1}, while for eskolaite the peak positions are 602, 544, 392, 345, and 306 cm^{-1}. The most evident difference in the spectrum of the mixed oxide $FeCrO_3$ with respect to those of the parent binary oxides is the detection, in the former case, of a very strong band in the region 700–500 cm^{-1}, definitely absent for pure oxides. According to McCarty and Boehme (10) and McCarty (24), this feature cannot be due to a scattering from the magnetic structure of the metal oxide. The comparison with the Raman spectra of the other mixed oxides can allow an interpretation for this feature. The Raman spectra of $NiTiO_3$ and $CoTiO_3$ (Fig. 4) show a strong parallelism with that of the isostructural compound geikielite $MgTiO_3$ (Table 3), reported by White (25). All present an extremely strong feature in the region 750–600 cm^{-1}, which is certainly due to a true vibrational peak.

To get information from these spectra, we should take into account some details of the corundum-type and derived structures (1, 26, 27). The corundum-type structure of α-A_2O_3 sesquioxides is basically constituted by a hexagonal close-packed array of oxide ions, with trivalent A cations occupying two-thirds of the octahedral holes. The distribution of cations in the 0001 hexagonal basal plane is reported in Fig. 5. This structure belongs to the $R\bar{3}c = D_{3d}^6$ space group. At least three different cation orderings can occur when half of the A cations of a corundum-type sesquioxide are substituted for by a B cation, giving rise to an ABO_3 hexagonal mixed oxide. Obviously,

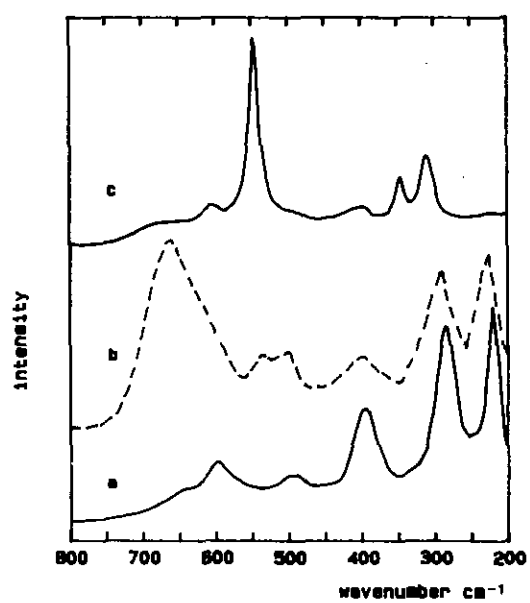

FIG. 3. Laser–Raman spectra of (a) α-Fe_2O_3, (b) $FeCrO_3$, and (c) α-Cr_2O_3.

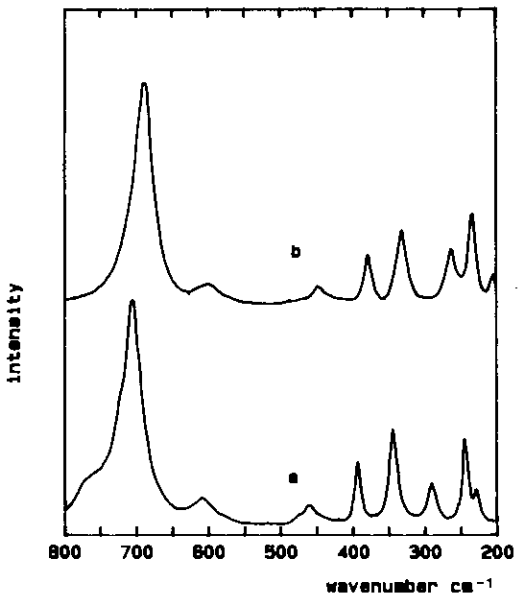

FIG. 4. Laser–Raman spectra of (a) $NiTiO_3$ and (b) $CoTiO_3$.

A and B cations can be both trivalent, or A divalent and B tetravalent (as in ilmenite-type titanates), or, finally, A monovalent and B pentavalent, respectively. Ilmenite-type mixed oxides, such as $FeTiO_3$ (ilmenite) and the isostructural compounds $CoTiO_3$, $NiTiO_3$, and $MgTiO_3$, are characterized by the segregation of the different cations A and B into different planes parallel to the 0001 hexagonal basal plane, as shown in Fig. 6. This lowers the symmetry, with the disappearance of the three glide planes typical of the $R\bar{3}c$ space group, but with retention of the center of symmetry and of the trigonal axis, giving rise to the $R\bar{3} = C_{3i}^2$ space group. In contrast, in the case of the low-temperature form of $LiNbO_3$, the A and B cations alternate in all planes and directions. The cations distribution in the 0001 hexagonal basal plane is shown

TABLE 3
Raman Peak Position (cm^{-1}) for Ilmenite-Type Mixed Oxides

$MgTiO_3$[a]	$CoTiO_3$	$NiTiO_3$	$FeCrO_3$
(780)		(760)	
720	688	705	655
649	602	608	600
491	450	458	500
404	379	389	393
359			
332	332	338	289
312			
287	263	284	
258			
230	233	238	220
211	204	226	
165		183	

[a] Ref. (25).

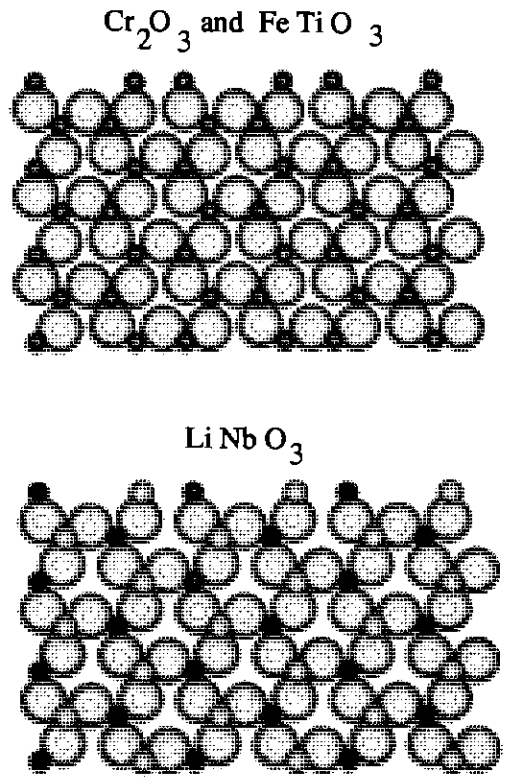

FIG. 5. Representation of the cation ordering in the 0001 hexagonal planes (111 in the rhombohedral system) of corundum-type α-Cr_2O_3, ilmenite-type structures (Fe–TiO_3, ilmenite) and low-temperature $LiNbO_3$. Big balls, oxide ions; small balls, cations.

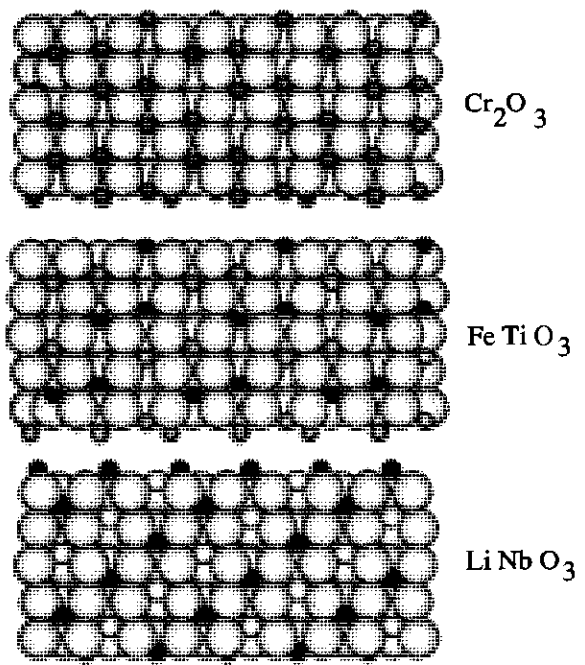

FIG. 6. Representation of the cation ordering along the c axis of corundum-type α-Cr_2O_3, ilmenite-type structures ($FeTiO_3$, ilmenite), and low-temperature $LiNbO_3$. View of the $1\bar{1}0$ plane (rhombohedral system). Big balls, oxide ions; small balls, cations.

in Fig. 5, while the distribution along the c axis is shown in Fig. 6. In this case, the glide planes are retained but the center of symmetry is lost. Thus, the space group is $R3c = C_{3v}^6$.

In all cases, the rhomohedral unit cell contains six oxide anions and four cations (two ABO_3 or A_2O_3 molecules). In Fig. 7, the idealized rhombohedral unit cells of the three structures are compared.

According to the factor group analysis for corundum (28), seven Raman active modes ($2\,A_{1g} + 5\,E_g$) and six IR active modes ($2\,A_{2u} + 4\,E_u$) are expected, besides five inactive modes ($3\,A_{2g} + 2\,A_{1u}$) and the acoustic modes ($A_{2u} + E_u$). According to the presence of a center of symmetry and the "mutual exclusion rule," both IR and Raman active bands are not expected. In Table 4, the positions of the active modes of α-Fe_2O_3 and α-Cr_2O_3, as observed in single crystal measurements, are reported and can be compared with those we observed in our fine powders measurements (see above). Taking into account the superposition of some bands, we observe all the IR active fundamentals for α-Cr_2O_3 and at least the four highest frequencies of the six active fundamentals for α-Fe_2O_3. As for the Raman spectra, we only lost a few of the lowest frequency fundamentals, due to their weakness (10).

In the case of ilmenite-type compounds, the center of symmetry is retained, so the mutual exclusion principle is still valid. In this case, we expect ten Raman active modes ($5\,A_g + 5\,E_g$) and eight IR active modes ($4\,A_u + 4\,E_u$) with acoustic modes ($A_u + E_u$) without any inactive mode. We observe for $NiTiO_3$ and $CoTiO_3$ at least six of eight IR active fundamentals and nine of ten Raman active fundamentals. The fundamentals lost can be assigned to low-intensity modes or are superimposed to other ones.

Finally, in the case of the $LiNbO_3$ structure, the center of symmetry is lost, and this results in both IR and Raman active modes; in particular, thirteen both IR and Raman active modes are expected ($4\,A_1 + 9\,E$) with five inactive modes (A_2) and the acoustic modes ($A_2 + E$).

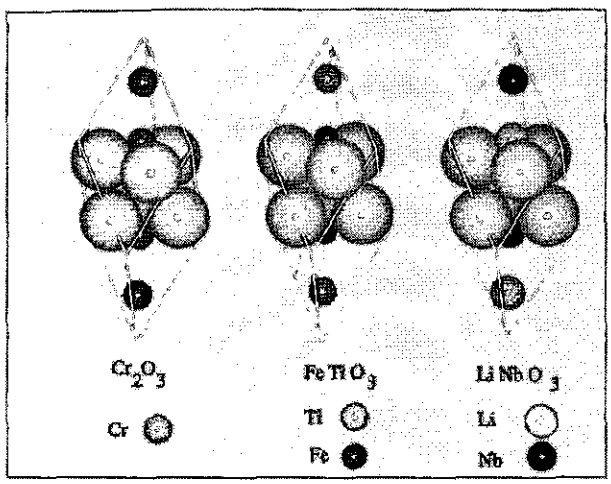

FIG. 7. Schematic representation of the unit cells of rhombohedral–hexagonal oxides and of cation ordering in them.

TABLE 4
IR and Raman Active Fundamentals in Corundum-Type Sesquioxides[a]

Symmetry	α-Fe_2O_3	α-Cr_2O_3
A_{2u}	299	538
	526	613
E_u	227	417
	236	444
	437	532
	524	613
A_{1g}	225	266
	498	547
E_g	250	235
	293	290
	299	352
	412	528
	613	617

[a] Refs. (16, 21–23).

The detection for $FeCrO_3$ of Raman bands that are not observed in the spectra of the parent sesquioxides definitely provides evidence for cation ordering in this structure. The comparison of the vibrational spectra of $FeCrO_3$ with those of the ilmenite-type compounds under study definitely suggests that an ilmenite-type cation ordering probably occurs in $FeCrO_3$. Different cation ordering, such as that of the $LiNbO_3$ structure, seems to be excluded because: (i) much more fundamentals should be expected in both IR and Raman spectra; (ii) the mutual exclusion rule, clearly fulfilled for $FeCrO_3$, without any correspondence of IR and Raman maxima, suggests a centrosymmetric structure, in contrast to what is expected for the noncentrosymmetric $LiNbO_3$, in which all modes are both IR and Raman active. In fact, the IR spectra of $LiNbO_3$ powders (29) and the IR and Raman spectra of $LiNbO_3$ monocrystals (30, 31) have been published and correspond to the forecasts, with the appearance of 13 fundamentals coinciding in IR and Raman spectra.

The most typical feature is the strong Raman mode observed near 700 cm^{-1} on both $FeCrO_3$ and ilmenite-type oxides. This mode is not observed at all on Fe_2O_3 nor on Cr_2O_3. According to our interpretation, this mode should be A_{2g} in corundum (inactive) and A_g in ilmenite (Raman active). It seems unlikely that this band arises from an IR active mode that becomes also Raman active, as proposed by McCarty (10, 24). In fact, the sesquioxides do not show fundamental modes in this region, and the theory does not predict the activation in Raman of an IR active mode. The Raman mode near 700 cm^{-1} is the high-

est frequency fundamental for ilmenite-type compounds. Thus, this mode arises from the highest frequency vibrational mode of MO_6 octahedra that is the symmetric stretching mode (A_{1g} symmetry for regular O_h octahedra), just found near 700 cm^{-1} in the Raman spectra of many MO_6 octahedra (32, 33).

We can propose that the band observed near 700 cm^{-1} in the Raman spectra of $FeCrO_3$ and of ilmenite-type oxides is associated with a stretching mode in which the octahedra in successive planes of the 0001 family alternatively contract and expand. According to the C_3 axes of the corundum structure, this mode is expected to be A_{2g}, thus being inactive. In fact, half of the AO_6 octahedra expand when half contract, without any variation in the total polarizability (Raman inactivity) and in the dipole moment (IR inactivity). On the contrary, in the ABO_3 ilmenite structures, this mode is expected to become A_g, Raman active. In this case, in fact, because of the segregation of cations in different planes of the 0001 family, when AO_6 octahedra expand, BO_6 octahedra contract and vice versa, and polarizability changes upon this movement. In the case of the $LiNbO_3$-type structure, this mode is also expected to be inactive, because half of the AO_6 and half of the BO_6 octahedra contract when the other halves of them expand. This mode is A_2 for $LiNbO_3$-type structures.

The interpretation of the vibrational spectra of $FeCrO_3$ fine powders as being due to an ilmenite-type structure contrasts with the common opinion that cation ordering in the hexagonal ABO_3 structures only occurs if A and B have different oxidation states. In effect, the UV–visible spectrum of our $FeCrO_3$ fine powders (3) strongly suggests that both iron and chromium are in the trivalent state. However, although spectra similar to ours have also been recorded for samples prepared by solid state reaction (10), it is not excluded that the cation ordering we observe (perhaps in a metastable form) is the result of our coprecipitation procedure. To have better information on this, studies of the temperature effects on the IR and Raman spectra of $FeCrO_3$ are in progress.

CONCLUSION

Vibrational spectra suggest that $FeCrO_3$ fine powders are characterized by an ilmenite-type cation ordering ($R\bar{3} = C_{3i}^2$), although XRD data do not allow the evidencing of this superstructure of the corundum structure. In particular, this is evidenced clearly from the Raman spectra, in which a strong band absent on corundum-type compounds appears, as on ilmenite compounds. It is possible that Cr and Fe are not distinguishable by XRD because of the very similar scattering power of Cr and Fe and of the small crystal sizes of the powders, which are distinguished by vibrational spectroscopy, because of the significantly different Cr–O and Fe–O force constant.

ACKNOWLEDGMENT

This work has been supported in part by Murst (Rome).

REFERENCES

1. A. F. Wells, "Structural Inorganic Chemistry." Oxford Univ. Press (Clarendon), London/New York, 1975.
2. A. Muan and S. Somiya, *J. Am. Ceram. Soc.* **43,** 207 (1960).
3. G. Busca, G. Ramis, M. C. Prieto, and V. Sanchez Escribano, *J. Mater. Chem.* **3,** 665 (1993).
4. L. Lloyd, D. E. Ridler, and M. V. Twigg, *in* "Catalyst Handbook" (M. V. Twigg, Ed.), 2nd ed. Wolfe Pub., London, 1989.
5. E. H. Lee, *Catal. Rev. Sci. Eng.* 8, 285 (1973).
6. H. H. Kung and M. C. Kung, *Adv. Catal.* **33,** 159 (1985).
7. Y. Shimizu, S. Kusano, H. Kuwayama, K. Tanaka, and M. Egashira, *J. Am. Ceram. Soc.* **73,** 818 (1990); C. Cantalini and M. Pelino, J. Am. *Ceram. Soc.* **75,** 546 (1992).
8. S. C. Tjong, *Mater. Res. Bull.* **18,** 157 (1983).
9. D. J. Gardiner, C. J. Littleton, K. M. Thomas, and K. N. Strafford, *Oxid. Met.* **27,** 57 (1987).
10. K. F. McCarty and D. R. Boehme, *J. Solid State Chem.* **79,** 19 (1989).
11. G. Busca, V. Lorenzelli, V. S. Escribano, and R. Guidetti, *J. Catal.* **131,** 167 (1991).
12. G. Busca, V. Lorenzelli, and V. S. Escribano, *Chem. Mater.* **4,** 595 (1992).
13. G. Busca, G. Ramis, V. Lorenzelli, and R. J. Willey, *Langmuir* **9,** 1492 (1993).
14. Landolt-Bornstein, "Numerical Data and Functional Relationships in Science and Technology, Vol. 4, Magnetic and other Properties of Oxides." Springer–Verlag, Berlin, 1970.
15. C. J. Serna, J. L. Rendon, and J. E. Iglesias, *Spectrochim. Acta Part A* **38,** 797 (1982); C. J. Serna, M. Ocana, and J. E. Iglesias, *J. Phys. C.* **20,** 473 (1987).
16. S. Onari, T. Arai, and K. Kudo, *Phys. Rev. B.* **16,** 1717 (1977).
17. Sh. Yariv and E. Mendelovici, *Appl. Spectrosc.* **33,** 410 (1979).
18. B. Gillot, F. Bouton, F. Chassagneux, and A. Rousset, *J. Solid State Chem.* **33,** 245 (1980).
19. J. A. Gadsden, "Infrared Spectra of Minerals and Related Inorganic Compounds." Butterworths, London, 1975.
20. O. Yamaguchi, M. Morimi, H. Kawabata, and K. Shimizu, *J. Am. Ceram. Soc.* **70,** C97 (1987).
21. I. R. Beattie and T. R. Gilson, *J. Chem. Soc. A,* 980 (1970).
22. T. R. Hart, R. L. Aggarwal, and B. Lax, *in* "Proc. 2nd. Int. Conf. Light Scattering in Solids," p. 174. Flammarion, Paris, 1971.
23. T. R. Hart, S. B. Adams, and H. Temkin, "Proc. 3rd Int. Conf. Light Scattering in Solids," p. 259. Wiley, New York, 1976.
24. K. F. McCarty, *Solid State Commun.* **68,** 799 (1988).
25. W. B. White, *in* "The Infrared Spectra of Minerals" (V. C. Farmer, Ed.), p. 93. The Mineralogical Society, London, 1974.
26. B. G. Hyde and S. Andersson, "Inorganic Crystal Structures." Wiley, New York, 1989.
27. J. C. Decius and R. M. Hexter, "Molecular Vibrations in Crystals," McGraw–Hill, New York, 1977.
28. S. Bhagavantam and T. Venkatarayudu, *Proc. Indian Acad. Sci. Sect. A* **9,** 224 (1939).
29. M. I. Diaz-Guemes, T. Gonzalez Carreno, and C. J. Serna, *Spectrochim. Acta Part. A* **45,** 589 (1989).
30. A. S. Barker, Jr. and R. Loudon, *Phys. Rev.* **158,** 433 (1967).
31. I. P. Kaninow and W. D. Johnston, Jr., *Phys. Rev.* **160,** 519 (1967).
32. K. Nakamoto, "Infrared and Raman Spectra of Inorganic and Coordination Compounds, 4th ed." Wiley, New York, 1986.
33. G. Blasse, *Spectrochim. Acta Part A* **32,** 1793 (1976).